

# Thermal, radioactive and magnetic properties of the lavas of the Mt Melbourne Volcanic Field (Victoria Land, Antarctica)

---

---

Vincenzo Pasquale, Massimo Verdoya, Paolo Chiozzi and Egidio Armadillo

*Dipartimento per lo Studio del Territorio e delle sue Risorse, Settore di Geofisica, Università di Genova, Italy*

## Abstract

We present the results of measurements of physical properties carried out on mafic lavas from the Mt Melbourne Volcanic Field, useful for interpretation of geophysical surveys designed to shed light on the structure of the crust. The thermal conductivity is comparable to that of glass and shows a clear negative dependence on porosity. The volume heat capacity and the thermal diffusivity are less variable. The concentration of the thermally important natural radioactive isotopes was determined by gamma-ray spectrometry. Lavas denoted a rather low heat-production rate, and the largest concentration of heat-producing elements (potassium, uranium, thorium) was found in the trachyte samples. The magnetic susceptibility is more variable than the other physical properties and, among the several iron-titanium oxides, it appears primarily controlled by the ulvöspinel-magnetite solid solution series.

**Key words** *petrophysics - thermal and magnetic properties - radioactive heat production - volcanic rocks*

## 1. Introduction

The Mt Melbourne Volcanic Field, forming the youngest volcanic system of the McMurdo Volcanic Group, is located in the Victoria Land (Antarctica) at the eastern flank of the Ross Sea rift. The latter is part of the West Antarctic Rift System, one of the largest tectonic provinces of the Earth with extended continental crust (*e.g.* Storti *et al.*, 2008). Volcanic evidence shows

that rifting commenced after the break-up of Australia and Antarctica about 100 Ma and was active until the middle Cenozoic (Cande *et al.*, 2000; Hamilton *et al.*, 2001). General overviews of volcanological, stratigraphical and other field aspects as well as geochemical information on individual volcanic fields of the McMurdo Volcanic Group are given by Kyle (1990) and Wörner (1999), whereas Armienti *et al.* (1991) and Rocholl *et al.* (1995) focus on rocks from the Mt Melbourne Volcanic Field (figs. 1 and 2).

This work falls within a program of geophysical research aimed at studying the supply system and zones of accumulation of magma in the crust of the McMurdo Volcanic Group.

We present the results of petrophysical properties useful to calibrate models of crustal structure. We carried out laboratory measurements of thermal and magnetic properties of lavas of the Mt Melbourne Volcanic Field. These properties were determined in connection with bulk density and porosity. A set of

---

*Mailing address:* Prof. Vincenzo Pasquale, Dipartimento per lo Studio del Territorio e delle sue Risorse, Settore di Geofisica, Università di Genova, Via Benedetto XV 5, I-16132 Genova, Italy; e-mail: pasquale@diptervis.unige.it

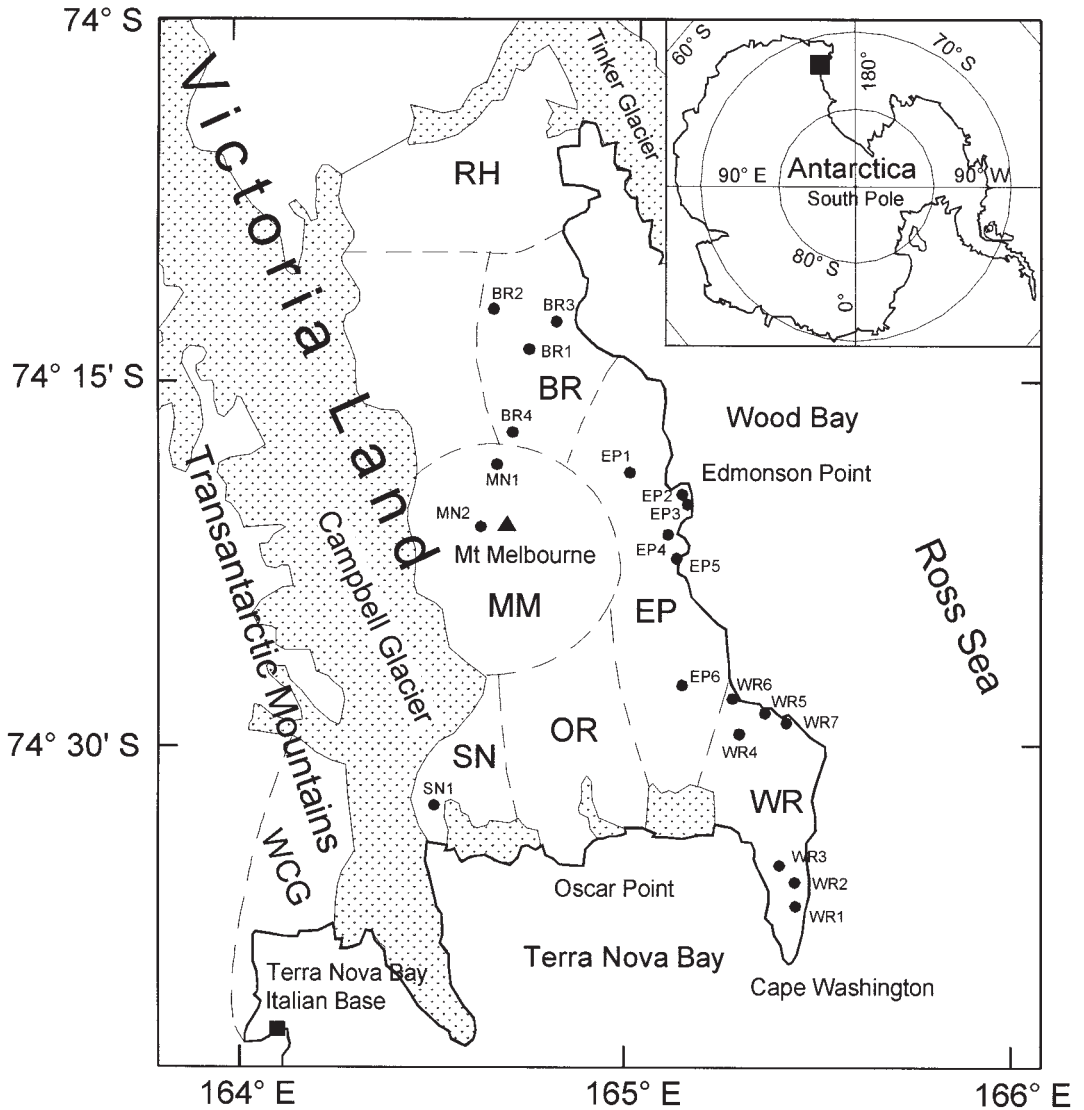


**Fig. 1.** Sketch map of the Mt Melbourne Volcanic Field showing position of sampling sites (see table I for sample codes and types of rocks). Sub-fields: WCG – West of Campbell Glacier, SN – Shield Nunatak, OR – Oscar Ridge, WR – Washington Ridge, EP – Edmonson Point, BR – Baker Rocks, RH – Random Hills, MM – Mt Melbourne summit.

gamma-ray spectrometry measurements were also carried out to determine the concentrations of uranium, thorium and potassium and the radioactive heat-production rate of the different rock types.

## 2. Sampling and laboratory procedure

Figure 1 shows the location of the sampling sites and the main sub-fields of the Mt Melbourne Volcanic Field. The presence of an ice

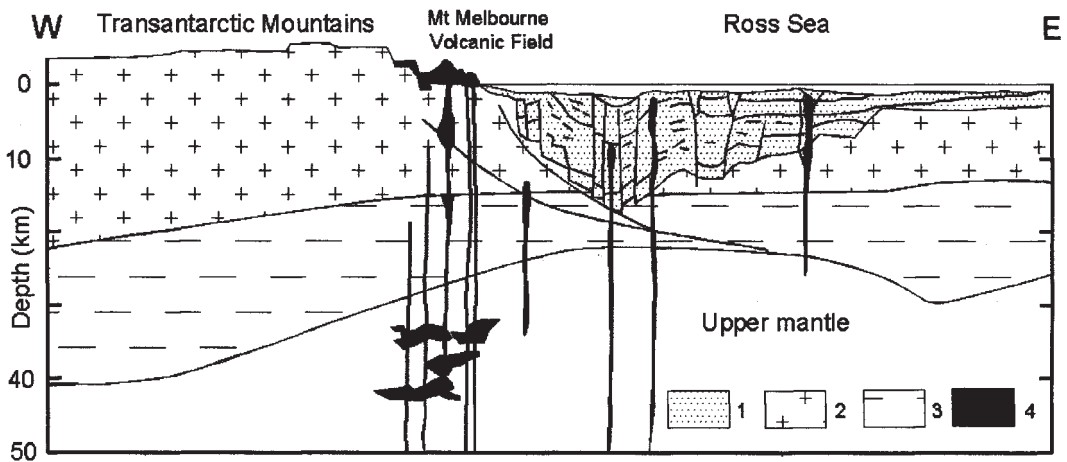


Fig. 2. Schematic cross-section of the lithosphere showing the transition from the Ross Sea rift to the Transantarctic Mountains, based on geophysical data, xenolith evidence and information from volcanic rocks (Wörner, 1999). 1. Sediments, 2. Upper crust, 3. Lower crust, 4. Mt Melbourne Volcanic Field.

sheet allowed sampling of the exposed volcanic rocks only in Washington Ridge, Edmonson Point, Baker Rocks, Shield Nunatak and Mt Melbourne summit sub-fields. As a whole, twenty samples were collected paying attention to avoid sampling of rocks with evident weathering. Table I presents the chemical composition for each sample obtained by means of inductively coupled plasma mass spectrometry at the Activation Laboratories LTD, Ontario (Canada), whereas fig. 3 depicts the alkali-silica diagram and the rock classification.

The Washington Ridge (WR) is formed by a line of sub-aerial scoria cones and tuff rings. All samples of lavas are characterized by the lack of feldspar phenocrysts and, with the exception of sample WR6, they have a chemical composition ranging from basanite to amphibole-bearing tephrite. In the Edmonson Point (EP) eruptive centres and scattered deposits of tuff-breccias and pillows show a complex association of different rock types; our lava samples range from tephritic to trachyandesitic composition. The Shield Nunatak (SN) area is formed by a cluster of subglacial eruptive centres with a flat-topped morphology; we recovered only one sample of basaltic composition. Lithotypes sampled at Baker Rock (BR) range from basan-

ites (BR1-BR3) to trachybasalt (BR4). The Mt Melbourne summit (MM) is a stratovolcano formed between 0.01-0.25 Ma, built on a base of trachytic lava flows and domes; samples are of trachyandesitic-trachytic to basaltic composition.

Thermal and magnetic properties of rock of the Mt Melbourne Volcanic Field were investigated according to standard procedures implemented at our laboratory. The thermal conductivity, thermal diffusivity and volume heat capacity measurements were carried out at room temperature by two devices: (i) an apparatus (PRC) devised by us (Pasquale, 1982 and 1983); (ii) a heat transfer analyzer (ISOMET) for measurements under transient regime, manufactured by Applied Precision Ltd. (Bratislava, Slovakia). The heat-production rate and the magnetic susceptibility were obtained from measurements with a gamma-ray spectrometer (GRS) and a magnetic susceptibility system (MS2) manufactured by EG & G-Ortec (Usa) and Bartington Instruments (Witney, Oxford, England), respectively.

The PRC apparatus allows accurate determinations of thermal conductivity of solid material in the range  $0.3-11 \text{ W m}^{-1} \text{ K}^{-1}$ . The total relative uncertainty, as shown by experiments

**Table I.** Chemical composition (in mass %) obtained from inductively coupled plasma mass spectrometry (ICP-MS) and rock type (see fig. 1 for sample location).

Sample	SiO <sub>2</sub>	TiO <sub>2</sub>	Al <sub>2</sub> O <sub>3</sub>	Fe <sub>2</sub> O <sub>3</sub>	FeO	MnO	MgO	CaO	Na <sub>2</sub> O	K <sub>2</sub> O	P <sub>2</sub> O <sub>5</sub>	S	Total	Rock type
WR1	43.65	3.27	13.51	3.99	9.31	0.21	7.96	8.67	4.35	1.66	1.04	0.08	97.70	Basanite
WR2	42.29	3.98	12.68	4.29	10.11	0.18	8.43	10.48	3.75	1.95	0.83	0.73	99.70	Basanite
WR3	45.05	3.31	14.06	3.00	9.50	0.21	7.32	8.41	4.54	2.08	1.16	0.03	98.67	Basanite
WR4	45.62	2.72	14.42	3.50	11.08	0.24	3.96	8.02	4.30	1.77	1.79	0.04	97.46	Basanite
WR5	44.92	3.64	14.20	3.96	8.79	0.20	7.42	8.87	4.66	2.22	0.83	0.06	99.77	Basanite
WR6	46.68	2.55	15.37	3.38	9.08	0.21	5.67	9.08	4.24	1.47	0.97	0.02	98.72	Trachybasalt
WR7	42.30	3.77	15.22	4.36	10.00	0.21	5.30	9.21	3.36	1.07	1.15	0.06	96.01	Basanite
EP1	50.40	2.04	16.64	3.03	9.09	0.25	2.79	6.72	5.34	2.32	1.01	0.05	99.68	Basaltic trachyandesite
EP2	44.62	4.11	15.71	4.09	10.01	0.22	4.84	10.04	3.70	1.15	1.21	0.11	99.81	Tephrite
EP3	58.83	0.99	16.37	3.11	6.05	0.23	0.89	3.70	5.80	3.70	0.31	0.02	99.80	Trachyandesite
EP4	48.34	2.57	16.52	3.36	9.09	0.23	3.64	8.10	4.61	1.89	1.21	0.06	99.62	Trachybasalt
EP5	48.67	2.68	15.52	4.09	9.10	0.25	3.46	7.72	4.53	2.14	1.34	0.03	99.53	Trachybasalt
EP6	46.65	2.87	15.29	3.08	9.56	0.21	6.46	9.66	4.02	1.50	0.97	0.02	99.89	Trachybasalt
SN1	45.07	2.95	12.67	2.80	9.92	0.18	10.55	11.78	2.56	0.66	0.69	0.09	99.92	Basalt
BR1	42.45	2.04	13.40	2.82	7.25	0.19	6.89	8.16	4.57	1.82	0.93	0.05	90.57	Basanite
BR2	43.39	3.42	16.45	4.26	8.91	0.19	6.13	10.81	3.08	1.04	0.98	0.06	98.72	Basanite
BR3	44.73	3.33	13.63	4.83	8.31	0.18	10.12	9.34	3.36	1.14	0.59	0.03	99.59	Basanite
BR4	48.57	2.75	14.82	2.86	11.36	0.26	3.44	7.77	4.50	1.95	1.49	0.03	99.80	Trachybasalt
MM1	61.18	0.30	16.66	2.51	3.77	0.21	0.11	1.29	6.35	5.58	0.11	0.03	98.10	Trachyte
MM2	47.02	3.96	19.76	2.82	7.62	0.14	2.04	6.66	2.98	1.06	1.01	0.04	95.11	Basalt

performed on materials with well-known thermal properties, is less than 3%. Reproducibility of measurements on various rock samples is within  $\pm 2\%$ . PRC requires the sample to be prepared in cylindrical shape and clamped between two cylindrical copper blocks by a screw. The whole apparatus is initially kept at the same temperature, then the lower block is cooled and the temperature of the blocks is continuously recorded with thermocouples. When

a uniform temperature gradient is established within the stack of elements, the thermal conductivity of the sample is determined, the heat capacity of the upper block of copper and of the sample being known.

ISOMET uses a dynamic measurement method which allows simultaneous determinations of conductivity, diffusivity and volume heat capacity. The measurement range is  $0.02-6 \text{ W m}^{-1}\text{K}^{-1}$  for conductivity and  $0.04-4 \cdot 10^6 \text{ J}$

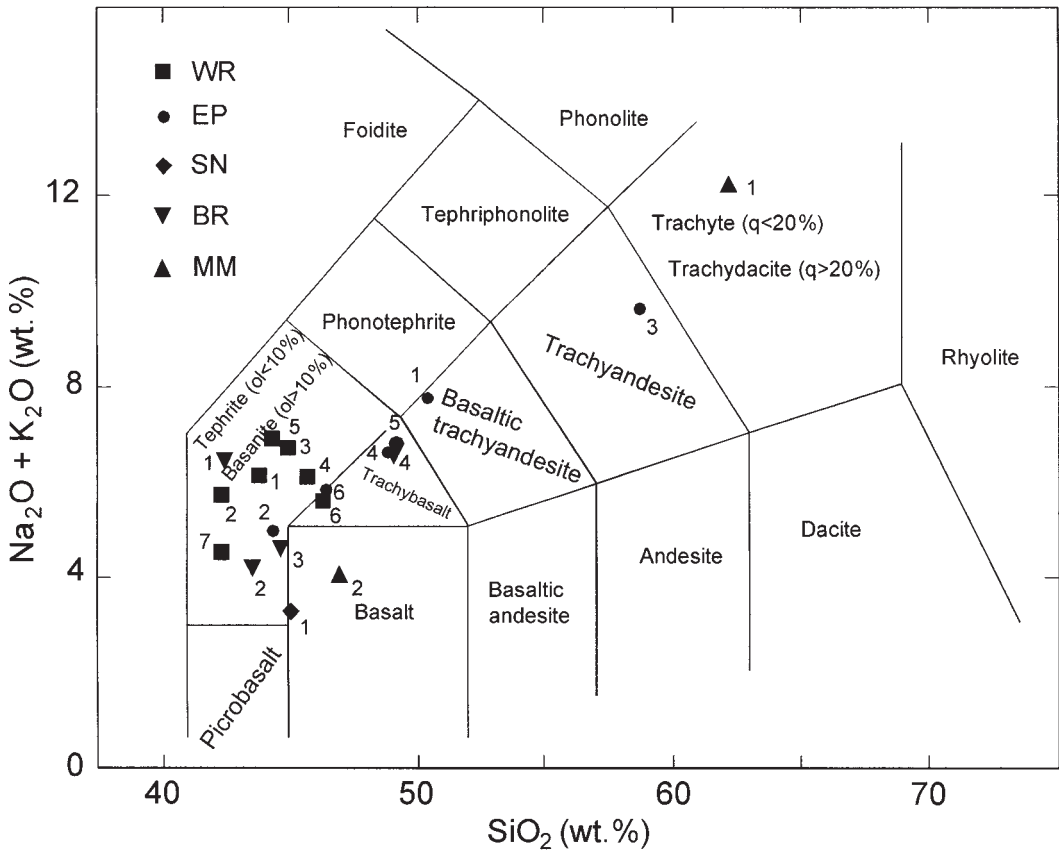


**Fig. 3.** Total alkali content ( $Na_2O + K_2O$ ) vs.  $SiO_2$ . Numbers at each data point correspond to those listed in table I. ol = olivine and q = quartz.

$m^{-3}K^{-1}$  for volume heat capacity, while reproducibility is 3% for both parameters, and the experimental relative error is less than 5%. Sample preparation for the ISOMET procedure is fast and only requires the rock to be cut and smoothed to obtain a flat surface. Interchangeable probes, calibrated for different ranges of thermal conductivity, are directly put on the sample surface. Thermal parameters are inferred from the increase in temperature with time at the sample surface due to heat flow released by a planar heat source.

The GRS consists of a scintillation detector (a  $7.62\text{ cm} \times 7.62\text{ cm}$  NaI(Tl) crystal with resolution about 7%) and a 2048 channel analyser.

The counting time for each sample was 5400 s. Based on counting statistics, the relative standard uncertainty on U, Th and K determinations are, in percent, 3.5, 2.4 and 1.2, respectively. For ultrabasic rocks with exceptionally low radioelement concentration the error may increase to 20%. For a sample weighing 0.750 kg, the detection limits are 0.1 ppm for U, 0.2 ppm for Th, and 0.02% for K (Chiozzi *et al.*, 2000a).

The MS2 system measures the magnetic susceptibility on samples (cores or powders) of 15 ml. It can be used for investigations of magnetic mineralogy and grain size and for determination of the Curie transition temperature. The relative uncertainty in the determinations is

**Table II.** Bulk density ( $\rho$ ), porosity ( $\sigma$ ), thermal conductivity ( $\lambda_1$  by ISOMET,  $\lambda_2$  by PRC), volumetric heat capacity ( $\rho \times c$ ) and thermal diffusivity ( $k$ ).

Sample	$\rho$ (kg m <sup>-3</sup> )	$\varphi$ (%)	$\lambda_1$ (W m <sup>-1</sup> K <sup>-1</sup> )	Std. Dev.	$\lambda_2$ (W m <sup>-1</sup> K <sup>-1</sup> )	Std. Dev.	$\rho \times c$ (J m <sup>-3</sup> K <sup>-1</sup> ) $\times 10^6$	Std. Dev.	$k$ (m <sup>2</sup> s <sup>-1</sup> ) $\times 10^{-6}$	Std. Dev.
WR1	2520	18	-	-	1.08	0.18	-	-	-	-
WR2	1440	55	0.53	0.02	0.60	0.09	1.61	0.02	0.33	0.01
WR3	2160	24	0.92	0.05	0.94	0.08	1.85	0.02	0.49	0.03
WR4	2240	23	0.84	0.01	-	-	1.82	0.01	0.46	0.01
WR5	2480	15	1.00	0.02	-	-	1.89	0.02	0.53	0.01
WR6	2470	17	0.86	0.01	-	-	1.89	0.02	0.46	0.01
WR7	2890	1	-	-	1.23	0.26	-	-	-	-
EP1	2740	9	1.04	0.01	-	-	1.94	0.02	0.54	0.01
EP2	2730	10	1.23	0.02	1.14	0.09	2.02	0.01	0.61	0.01
EP3	2370	13	0.82	0.01	-	-	1.88	0.01	0.33	0.01
EP4	2440	6	1.03	0.02	-	-	1.91	0.01	0.54	0.01
EP5	2750	1	1.02	0.02	-	-	1.71	0.02	0.60	0.01
EP6	2870	2	-	-	-	-	-	-	-	-
SN1	3030	1	1.38	0.06	-	-	1.94	0.04	0.71	0.02
BR1	2000	12	-	-	0.97	0.15	-	-	-	-
BR2	2660	12	1.19	0.06	-	-	1.89	0.09	0.63	0.01
BR3	2770	10	0.99	0.03	-	-	1.73	0.03	0.57	0.01
BR4	2300	23	0.98	0.06	0.91	0.09	1.85	0.10	0.53	0.01
MM1	1740	34	0.55	0.01	0.48	0.16	1.81	0.05	0.30	0.01
MM2	2700	7	-	-	1.06	0.34	-	-	-	-

as low as 5%, and the sensitivity is  $2 \cdot 10^{-6}$  SI. Repeated measurements on standards revealed very low drift.

The system has a low operating frequency, so that measurements are not affected by sample conductivity.

Compact rock samples were first cut with diamond disk to obtain flat surfaces as required by thermal property determinations according

to the ISOMET procedure. The surface dimensions were at least 6 cm in diameter and the minimum thickness 2-3 cm. Samples were then cored with a head-diamond corer.

The core specimens, about 3 cm high and 2.5 cm in diameter, were used for the determinations with PRC and MS2. Less massive rocks which could not be cut were reduced to powder. This allowed both measurements of magnetic

**Table III.** Concentration of the heat-producing elements (U, Th, K), radioactive heat-production rate (RHP) and magnetic susceptibility ( $\chi$ ).

Sample	K (%)	Std. Dev.	U (ppm)	Std. Dev.	Th (ppm)	Std. Dev.	RHP ( $\mu\text{W m}^{-3}$ )	Std. Dev.	$\chi$ (SI units) $\times 10^{-5}$	Std. Dev.
WR1	1.54	0.04	2.2	0.1	8.8	0.4	1.23	0.06	4486	11
WR2	1.68	0.04	1.4	0.2	5.7	0.5	0.49	0.07	231	1
WR3	1.97	0.04	3.0	0.1	12.0	0.5	1.43	0.06	3622	5
WR4	1.56	0.04	1.2	0.2	5.3	0.4	0.68	0.07	898	18
WR5	1.92	0.04	2.5	0.1	10.0	0.5	1.39	0.07	4057	3
WR6	0.85	0.04	0.6	0.2	6.5	0.4	0.63	0.04	2096	2
WR7	0.78	0.03	0.7	0.2	2.7	0.3	0.47	0.07	494	4
EP1	2.00	0.04	2.2	0.2	8.2	0.5	1.34	0.07	1904	4
EP2	1.00	0.03	1.1	0.2	3.9	0.4	0.65	0.06	338	5
EP3	3.27	0.05	3.2	0.1	11.9	0.5	1.71	0.07	822	1
EP4	1.02	0.04	0.9	0.2	3.2	0.4	0.50	0.06	879	17
EP5	1.77	0.04	1.6	0.1	6.1	0.4	1.02	0.06	1764	6
EP6	1.30	0.04	1.5	0.2	4.8	0.4	0.89	0.07	1805	3
SN1	0.67	0.03	0.8	0.2	2.1	0.4	0.46	0.06	298	1
BR1	1.42	0.05	0.6	0.3	3.3	0.6	0.38	0.08	791	3
BR2	0.89	0.03	0.8	0.2	3.1	0.4	0.50	0.07	813	1
BR3	0.99	0.03	0.9	0.2	3.6	0.4	0.59	0.07	4617	2
BR4	1.66	0.04	1.7	0.1	7.4	0.5	0.94	0.06	2243	9
MM1	4.53	0.08	5.3	0.2	19.0	0.8	2.00	0.08	119	1
MM2	1.05	0.04	1.6	0.2	7.6	0.5	1.04	0.07	648	1

susceptibility and GRS analyses to determine the concentration of heat-producing isotopes. A volume of 500 cm<sup>3</sup>, corresponding to rock mass ranging from 0.650 to 0.850 kg, was adopted for spectrometric measurements.

Moreover, bulk density and porosity were determined for all the samples. Thermal, GRS and magnetic measurements were carried out on five specimens obtained from each rock sample.

### 3. Results and discussion

Table II summarises the results of bulk density, porosity and thermal parameters. Thermal conductivity varied from 0.48 W m<sup>-1</sup>K<sup>-1</sup> (trachyte MM1) to 1.38 W m<sup>-1</sup>K<sup>-1</sup> (basalt SN1). For the five samples investigated with both PRC and ISOMET, the results are quite coherent, as the maximum difference between the two methods is close to the instrumental error (0.1 W m<sup>-1</sup>K<sup>-1</sup>).

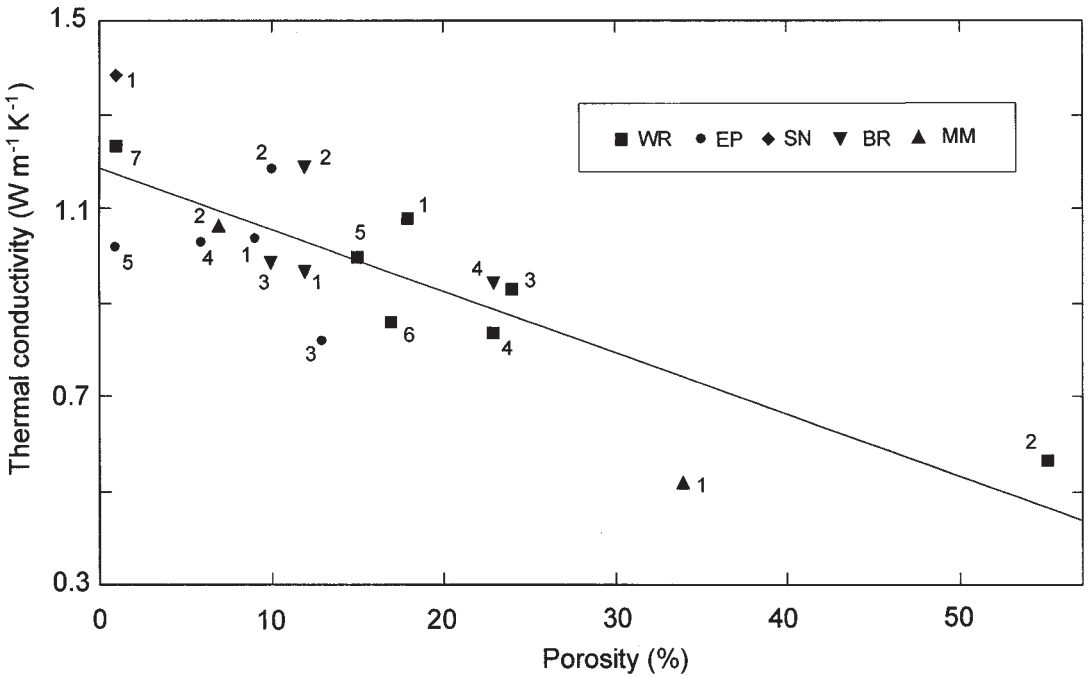


Fig. 4. Thermal conductivity values versus porosity.

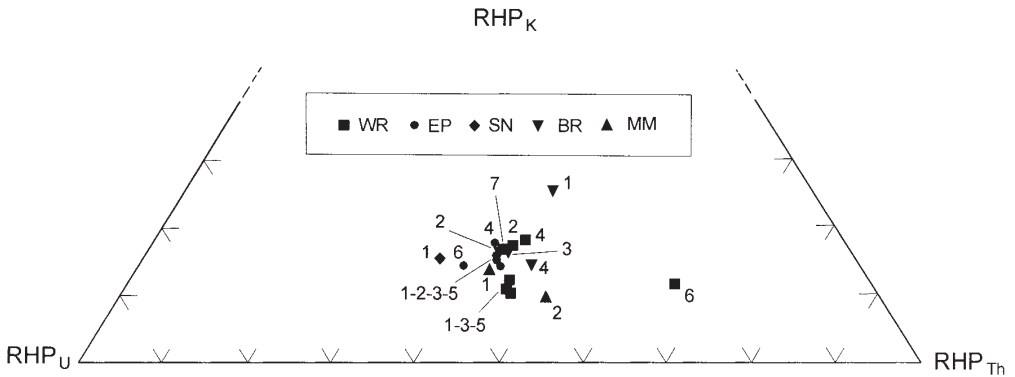


Fig. 5. Relative contribution of U, Th and K to the radioactive heat-production rate.

On the average, the volumetric heat capacity and the diffusivity are  $1.85 (\pm 0.10) 10^6 \text{ J m}^{-3} \text{ K}^{-1}$  and  $0.51 (\pm 0.12) 10^{-6} \text{ m}^2 \text{ s}^{-1}$ , respectively. Since the chemical composition is relatively homogeneous, thermal conductivity is mainly controlled by porosity. Figure 4 clearly points out a

linear decrease of this parameter with the increase in porosity, whose maximum value (55%) was found for WR2 (basanite).

The radioactive elements that mostly contribute to the internal heat generation are uranium, thorium and potassium. These elements



were determined by the three window method. Details on the adopted procedure and the system calibration are given by Chiozzi *et al.* (1998; 2000a and 2000b). In general, this method involves the detection of the gamma-radiation emission in the decay of  $^{214}\text{Bi}$  ( $^{238}\text{U}$  series),  $^{208}\text{Tl}$  ( $^{232}\text{Th}$  series), and  $^{40}\text{K}$ . However, it must be stressed that secular radioactive equilibrium in the decay series is necessary for appropriate measurements. This condition is generally fulfilled in  $^{40}\text{K}$  and  $^{232}\text{Th}$  series while problems may arise for uranium, where a minimum age of 0.3 My is required for  $^{226}\text{Ra}$  equilibrium.

The age of some volcanic sub-fields of Mt Melbourne is as young as 0.25 My. This means that secular equilibrium between U and its decay products might not be fulfilled in all the rock sampled. To bypass this problem, the gamma-ray spectrum region comprised between 0.03 and 0.10 MeV was investigated, instead of the higher energy photo-peak of  $^{214}\text{Bi}$  (1.76 MeV) (Ketcham, 1996). Chiozzi *et al.* (2000b) tested this approach on volcanic rocks younger than 0.3 My by comparing results from the NaI(Tl) spectrometer with a semiconductor (HPGe) detector, and they found that use of the low energy window can remarkably reduce the uncertainty in the U determination. In this low-energy region, there are a number of gamma rays produced by the decay of  $^{234}\text{Th}$ . This radioelement can be safely assumed to be in secular equilibrium with  $^{238}\text{U}$  as its half-life is only 24.1 days, and therefore it could have a different activity from post- $^{226}\text{Ra}$  daughter products, like  $^{214}\text{Bi}$ . As the NaI(Tl) scintillation detector does not have sufficient resolution for reliable identification of individual peaks in this region of low energy, it was necessary to operate with a relatively wide window, ranging from 0.010 to 0.123 MeV.

The results of GRS analyses are shown in table III. Generally, lava samples denoted rather low radioelement concentrations. The largest concentration of heat producing elements (K, U and Th) was found in the trachytic sample MM1 (4.53%, 5.3 ppm and 19.0 ppm, respectively), whereas SN1 (basalt) resulted in the poorest in K and Th (0.67% and 2.1 ppm, respectively). The lowest concentrations of U (0.6

ppm) were obtained for BR1 (basanite) and WR6 (trachybasalt). If one neglects WR6, the Th/U ratio is  $3.93 \pm 0.59$ , *i.e.* not significantly different from the average value found in the literature.

If the rock density is known, the radioactive heat-production rate RHP due to the decay of  $^{235}\text{U}$ ,  $^{238}\text{U}$ ,  $^{232}\text{Th}$  and  $^{40}\text{K}$  can be calculated from the uranium and thorium concentrations (see Chiozzi *et al.*, 2002 for details). Considering the relative standard uncertainties and the detection limits of the GRS determinations, the resulting error on RHP is  $0.1 \mu\text{W m}^{-3}$ . The major effect is due to U, whereas the accuracy and the detection limit of K are almost negligible in this regard.

The radiogenic heat productivity of the analyzed lavas is relatively low, as a consequence of the low concentration of heat-producing radioelements (table III). RHP ranges from a minimum of  $0.38 \mu\text{W m}^{-3}$  for BR1 (basanite) to a maximum of 2.00 for MM1 (trachyte). The relative contribution supplied by U, Th and K to the radioactive heat-production rate is shown in fig. 5.

The results of magnetic susceptibility measurements are also shown in table III. Measured values, which range from 0.001 (trachyte MM1) to 0.046 SI units (basanite BR3), mainly depend on the content of iron-titanium oxides. The oxides of interest in rock magnetism form a ternary system with FeO, Fe<sub>2</sub>O<sub>3</sub> and TiO<sub>2</sub> as the end-members (fig. 6). The most interesting minerals in this system are wüstite (Fe<sub>1-x</sub>O), magnetite (Fe<sub>3</sub>O<sub>4</sub>), hematite ( $\alpha$ -Fe<sub>2</sub>O<sub>3</sub>), maghemite ( $\gamma$ -Fe<sub>2</sub>O<sub>3</sub>), pseudobrookite (Fe<sub>2</sub>TiO<sub>5</sub>), ferropseudobrookite (FeTi<sub>2</sub>O<sub>5</sub>), ilmenite (FeTiO<sub>3</sub>), and ulvöspinel (Fe<sub>2</sub>TiO<sub>4</sub>). There are three fundamental solid-solution series in this system: the ulvöspinel-magnetite series with an inverse spinel structure, the rhombohedral hematite-ilmenite series, and the orthorhombic pseudobrookite-ferropseudobrookite series (Petersen, 1976; Hunt *et al.*, 1995). Figure 6 shows the iron-titanium oxides for the examined lavas together with the major solid-solution series. The lava magnetic components are clustered round the ulvöspinel-magnetite solid solution series [xFe<sub>2</sub>TiO<sub>4</sub>(1 - x)Fe<sub>3</sub>O<sub>4</sub>] of x-value ranging from 0.5 to 0.7, as the most abundant mineral component responsible for the magnetic susceptibility.

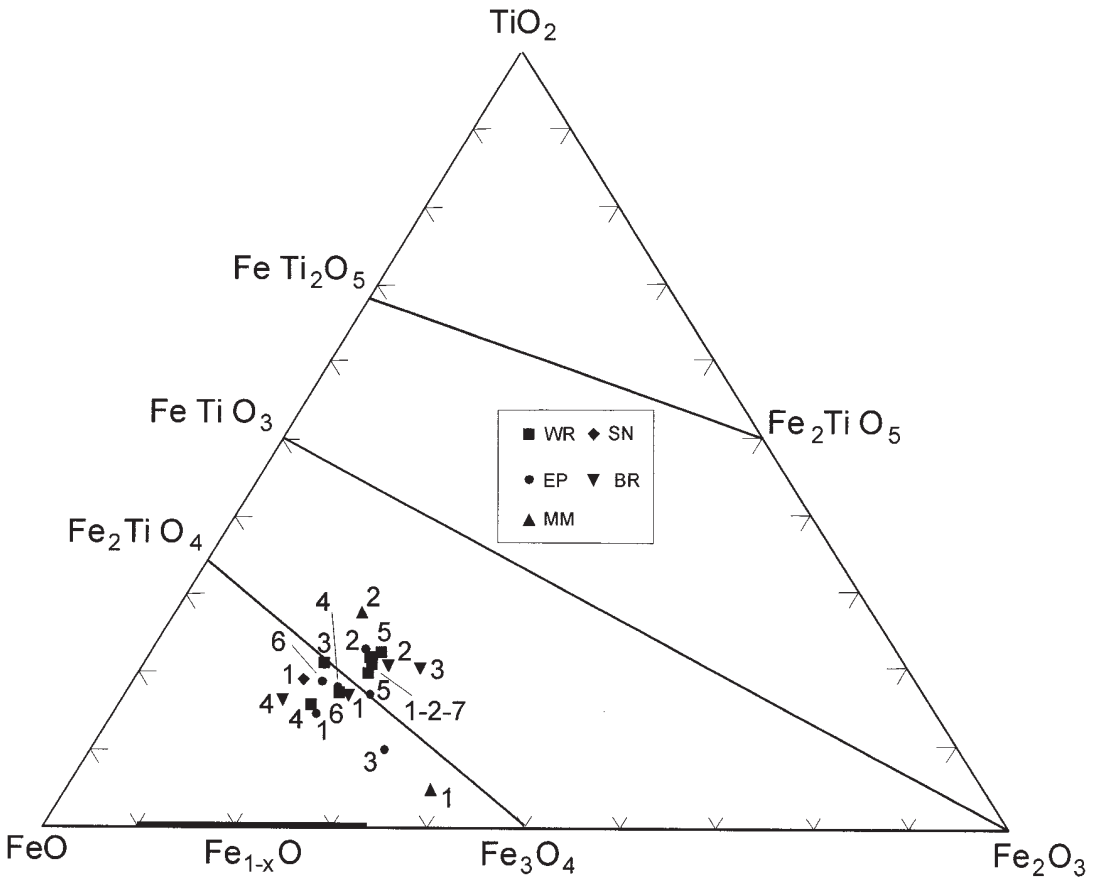


Fig. 6. Composition of the titanomagnetites of the investigated lavas.

Many titanomagnetites are slightly oxidized towards the titanohematite line or reduced.

#### 4. Conclusions

We identified the thermal and magnetic properties, together with density and porosity, of some mafic lavas representative of the Mt Melbourne Volcanic Field. This information is of basic importance for interpretation of gravity and magnetic anomalies, and is essential for future studies on the thermal structure of the area. Thermophysical properties reflect the ef-

fects of various geological processes acting during and after lava formation.

The thermal conductivity of lavas is comparable to that of glass and diminishes till it halves with the increase in porosity. Gamma-ray spectrometry results show low concentrations of radioactive elements and thus a low radioactive heat-production rate. For almost all the lava samples analyzed, the thorium/uranium ratio indicates no process of post-magmatic alteration.

Titanomagnetites appear to be the most abundant mineral components responsible for magnetic susceptibility.

## Acknowledgements

The authors thank Giorgio Caneva for his field work and support in laboratory measurements.

## REFERENCES

- ARMIENTI, P., L. CIVETTA, F. INNOCENTI, P. MANETTI, A. TRIPODO, L. VILLARI and G. VITA (1991): New petrological and geochemical data on Mt. Melbourne Volcanic Field (northern Victoria Land, Antarctica): II. Italian Antarctic Expedition, *Mem. Soc. Geol. It.*, **46**, 397-424.
- CANDE, S.C., J.M. STOCK, R.D. MULLER and T. ISHIHARA (2000): Cenozoic motion between East and West Antarctica, *Nature*, **404**, 145-150.
- CHIOZZI P., V. PASQUALE and M. VERDOYA (1998): Ground radiometric survey of U, Th and K in the Lipari Island, Italy, *J. Appl. Geophys.*, **38**, 209-217.
- CHIOZZI P., P. DE FELICE, V. PASQUALE and M. VERDOYA (2000a): Practical applicability of field radiometric analyses, *Applied Radiation and Isotopes*, **53**, 215-220.
- CHIOZZI, P., P. DE FELICE, A. FAZIO, V. PASQUALE and M. VERDOYA (2000b): Laboratory application of NaI(Tl)  $\gamma$ -ray spectrometry to studies of natural radioactivity in geophysics, *Applied Radiation and Isotopes*, **53**, 127-132.
- CHIOZZI P., V. PASQUALE and M. VERDOYA (2002): Heat from radioactive elements in young volcanics by  $\gamma$ -ray spectrometry, *J. Volcanology and Geothermal Research*, **119**, 205-214.
- HAMILTON R.J., B.P. LUYENDYK, C.C. SORLIEN and L.R. BARTEK (2001): Cenozoic tectonics of the Cape Roberts rift basin and Transantarctic Mountains front, southwestern Ross Sea, Antarctica, *Tectonics*, **20**, 325-342.
- HUNT, C.P., B.M. MOSKOWITZ and S.K. BANERJEE (1995): Magnetic properties of rocks and minerals, Rock physics and phase relations: a handbook of physical constant, edited by T.J. AHRENS, *Am. Geophys. Union, AGU Reference Shelf*, **3**, 189-204.
- KETCHAM, R.A. (1996): An improved method for determination of heat production with gamma-ray scintillation spectrometry, *Chem. Geol.*, **130**, 175-194.
- KYLE, P.R. (1990): McMurdo Volcanic Group, Introduction, in: *Volcanoes of the Antarctic Plate and Southern Oceans*, edited by W.E. LEMASURIER and J.W. THOMPSON, *Am. Geophys. Union, Antarctic Research Series*, **48**, 19-25.
- PASQUALE, V. (1982): A dynamic method for the rapid measurement of the thermal conductivity of rocks, *Workshop on Standard in Geothermics, Liblice (CSSR)*, June 1982, pp. 1-4.
- PASQUALE, V. (1983): *Sulla conducibilità termica delle rocce*, (Proceeding 2° Convegno del Gruppo Nazionale Geofisica della Terra Solida, C.N.R., Roma), pp. 765-775.
- PETERSEN, N. (1976): Notes on the variation of magnetization within basalt lavas flows and dikes, *Pageoph.*, **114**, 177-193.
- ROCHOLL, A., M. STEIN, M. MOLZAHN, S.R. HART and G. WÖRNER (1995): Geochemical evolution of rift magmas by progressive tapping of a stratified mantle source beneath the Ross Rift, Antarctica, *Earth Planet. Sci. Lett.*, **131**, 207-224.
- STORTI, F., M.L. BALESTRIERI, F. BALSAMO and F. ROSSETTI (2008): Structural and thermochronological constraints to the evolution of the West Antarctic Rift System in central Victoria Land, *Tectonics*, **27**, TC4012, doi:10.1029/2006TC002066.
- WÖRNER, G. (1999): Lithospheric dynamics and mantle sources of alkaline magmatism of the Cenozoic West Antarctic Rift System, *Global and Planetary Change*, **23**, 61-77.

(received November 21, 2008;  
accepted May 14, 2009)